



**HAL**  
open science

## Numerical analysis of both local geology and seismic directivity effects on ground motion prediction

S Touhami, F Gatti, F Lopez-Caballero

► **To cite this version:**

S Touhami, F Gatti, F Lopez-Caballero. Numerical analysis of both local geology and seismic directivity effects on ground motion prediction. 7th International Conference on Earthquake Geotechnical Engineering ( ICEGE 2019), Jun 2019, Rome, Italy. hal-03427399

**HAL Id: hal-03427399**

**<https://hal.science/hal-03427399v1>**

Submitted on 13 Nov 2021

**HAL** is a multi-disciplinary open access archive for the deposit and dissemination of scientific research documents, whether they are published or not. The documents may come from teaching and research institutions in France or abroad, or from public or private research centers.

L'archive ouverte pluridisciplinaire **HAL**, est destinée au dépôt et à la diffusion de documents scientifiques de niveau recherche, publiés ou non, émanant des établissements d'enseignement et de recherche français ou étrangers, des laboratoires publics ou privés.

# Numerical analysis of both local geology and seismic directivity effects on ground motion prediction

S. Touhami, F. Gatti & F. Lopez-Caballero

*Laboratoire MSS-Mat CNRS UMR 8579, CentraleSupélec Paris-Saclay University, France*

**ABSTRACT:** In this study, the influence of the 3D local geology and seismic directivity on the synthetic earthquake ground motion prediction is assessed on a real site. The studied site is located at Kefalonia Island (Greece). This site is well characterized and instrumented by several sensors. The numerical model of the earthquake scenario of the affected area is built-up and three small point-wise are simulated, changing the relative source-site position. Broad-band (0-5 Hz) synthetic wave-forms are obtained considering the presence of the 3D sedimentary basin of Koutavos. The different site amplification corresponding to three sources highlight the strong dependency on the wave direction. The impact of the sedimentary failures is also quantified at two different stations located inside and outside the basin.

## 1 INTRODUCTION

The seismic hazard is influenced by different effects, from the emission of waves during an earthquake to the studied site. This hazard depends on the heterogeneities of the fracture process at different scales, the wave propagation path and the site effects. At the regional level, the mechanisms of radiation during the rupture and its propagation in the earth's crust characterizing the hazard involve the determination of attenuation laws. On the other hand, at the local scale, the geomorphological conditions of a site can considerably intensify the strength of an earthquake by the amplification of the movement of the ground (Cruz-Atienza et al. 2016). The characterization and the consideration of these site effects, related to the soil conditions, are essential for the evaluation of the seismic risk. Site effects are related to the geometric structure of the soil and subsoil. Two types of structures are responsible for the main observed effects: the topography and the sedimentary fillings (e.g. during the 1985 Mexico City and 1995 Kobe earthquake (Pitarka et al. 1996)).

The importance of these local soil effects is well established, especially the effects of relief and sedimentary basins, which can generate large amplifications and significant spatial variations of ground motion and thus strongly influence long-term structures, such as large-scale bridges. At first, the 1D models made it possible to explain certain amplification effects. By their extreme simplicity of implementation and application, they are widely used in earthquake engineering (soil/structure interaction). But this 1D modelling is very limited, especially for the consideration of surface waves that can significantly amplify and lengthen the signals. 2D simulations have thus made it possible to highlight surface-wave reflection effects at the edge of a basin (Kawase 1996), as well as amplification effects related to a 2D mode resonance (Bard & Bouchon 1985). Numerous studies have shown the influence of the 3D basin structure on the seismic response, characterized by larger amplitudes and higher frequencies than the 1D and 2D responses. Predicting physics-based ground motion in a region characterized by complex geology is a challenge.

The simulation of ground motion created by an earthquake involves the numerical resolution of the equations of elastodynamics. Numerous numerical methods exist to simulate the wave propagation and have been developed lately. However, despite a good understanding of the physics and mathematics underlying the problem of ground motion simulation in complex geological framework, such simulations represent a real challenge. Three-dimensional simulations that consider

realistic models and cover the complete frequency band of interest are not yet sufficiently developed. Indeed, such studies imply the necessity to consider several aspects of the problem: large spatial expanses (allowing to capture all the phenomena of structural origin and those related to the source), a good resolution, constitutive laws capable of modelling the soil effects, seismic source modelling and many scenarios for a better characterization of the seismic hazard.

In this paper, the effect of local geology and seismic source directivity on predicted ground motion is studied numerically via the simulation of some seismic events in the site test installed at Kefalonia Island. For this study, the size of the considered computational model is  $27 \times 30 \times 50$  km and it can resolve wave propagation up to 5 Hz. The simulation concerns a Mw4.6 earthquake of the June, 04th 2016.

## 2 SEISMOTECTONIC AND GEOLOGICAL CONTEXT OF THE STUDIED AREA

For this study the Argostoli test site located at Kefalonia Island in Greece was selected. The study of this site is motivated by its geological configuration which makes it a basin favorable to the occurrence of 2D/3D site effects. The sedimentary basin (Koutavos) is located south of the capital of the island (Argostoli). It is located at the bottom of a lagoon and filled with quaternary and Pliocene detritic deposits (Cushing et al. 2016). It is a site of high seismicity because of its proximity to the Kefalonia Transform Fault (Sokos et al. 2016) which is a connection boundary close to the island of two subduction troughs: Hellenic Arc in the south and the Adriatic Fault Zone (Louvari et al. 1999) (Figure 1). The significant seismicity (in frequency and magnitude) allows to collect strong motions in a reduced time.

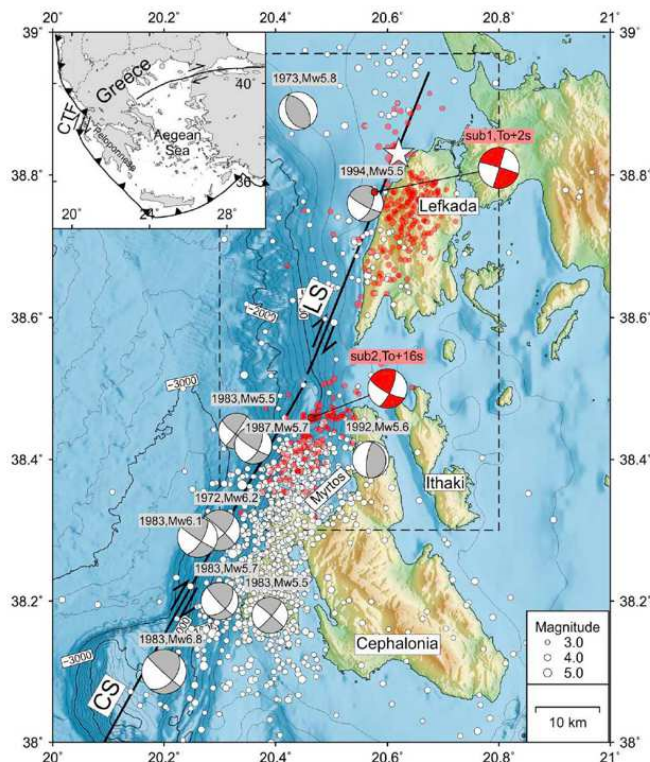


Figure 1.: Seismicity along the Cephalonia Segment and the Lefkada Segment of the Cephalonia Transform Fault Zone (bold black lines). (Sokos et al. 2015).

### 3 NUMERICAL MODELLING FOR 3D WAVE PROPAGATION

In this work the presented numerical simulations have been carried out by SEM3D code. It is a 3D Spectral Elements Method (Patera 1984, Mayday et al. 1989) code used to compute numerically the propagation of elastic waves in the solid or fluid medium. Among the advantages of SEM3D, its efficient and cost-effective massively parallel implementation (by Message Passing Interface, MPI) on large super-computers and its ability to accurately take into account 3D discontinuities such as the sediment-rock interface. The original core of the SEM3D software allowed to solve the wave propagation problem in any velocity model, including anisotropy and intrinsic attenuation.

The constructed 3D mesh is shown in Figure 2. The size of the studied model is :  $27 \times 30 \times 50$  km discretized using hexahedral mesh with characteristic element size of 130 m. This model can propagate frequencies up to 5 Hz.

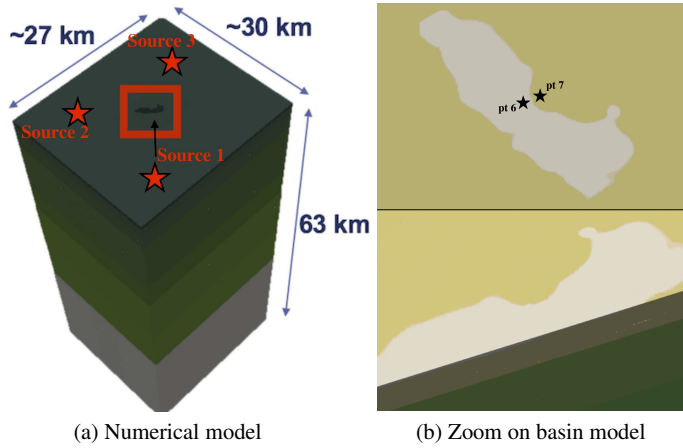


Figure 2.: Sketch of the numerical model of the studied Argostoli area including basin model.

#### 3.1 Geological model

Concerning the geological model, two velocity models was used in this work. For a regional scale, the adopted crustal velocity model of this region is the 1D profile proposed by Haslinger et al. 1999 (Table 1). Concerning the local scale, in order to study basin effects, a more refined geological model that has been obtained by Hollender et al. 2015 using in situ measurements is used (Table. 2).

Table 1. Values for 1D Crustal model proposed by Haslinger et al. 1999 for Ionian region.

Depth (km)	$V_p$ (km/s)	$V_s$ (km/s)	$Q_p$	$Q_s$
0.5	5.5	2.7	300	15
2.0	5.5	2.9	300	150
5.0	6.0	3.2	300	150
10.0	6.2	3.2	300	150
15.0	6.5	3.4	300	150
20.0	6.7	3.8	300	150
30.0	6.8	3.8	300	150
40.0	8.0	4.7	1000	500

Table 2. Values for velocity model proposed by Hollender et al. 2015 for Argostoli Area.

Depth (km)	$V_p$ (km/s)	$V_s$ (km/s)	$Q_p$	$Q_s$
0.0	2.0	0.6	300	150
0.03	2.4	1.0	300	150
0.4	4.6	2.7	300	150
1.0	6.0	3.2	300	150
2.0	6.2	3.2	300	150

### 3.2 Seismic source modelling

For this study the waves are generated by a source modelled by point-wise double-couple. It represents a magnitude  $M_w$  4.6. In order to evaluate the seismic source directivity effects, three locations of the same source was studied (Figure 3). The kinematic sources parameters are listed in Table 3. More detailed information about the data used to model the point source (orientation, magnitude) are available through the GEOFON Program website: <https://geofon.gfz-potsdam.de/data/alerts/2016/gfz2016kylx/mt.txt>

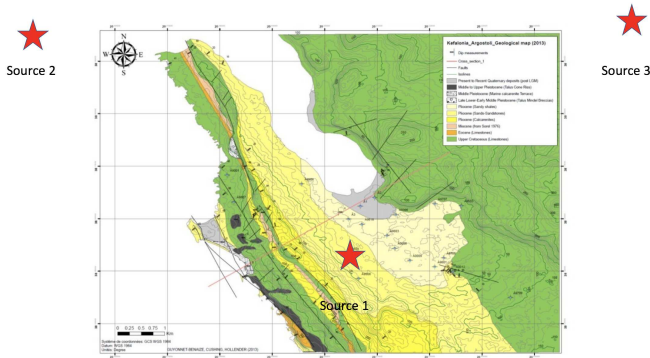


Figure 3.: Plan view of the Argostoli basin and the three studied seismic sources localization.

Table 3. Kinematic sources parameters for the simulations

Hypocenter ( $^{\circ}$ N, $^{\circ}$ E)	Depth (km)	Strike ( $^{\circ}$ )	Dip ( $^{\circ}$ )	Slip ( $^{\circ}$ )
38.15 $^{\circ}$ 20.50 $^{\circ}$	14	163	39	92
38.29 $^{\circ}$ 20.33 $^{\circ}$	14	163	39	92
38.30 $^{\circ}$ 20.65 $^{\circ}$	14	163	39	92

## 4 DISCUSSION OF RESULTS

Figure 4 shows the comparison of time history acceleration for source1 (red line), source2 (blue line), source3 (green line). This time histories are plotted for two receivers located inside the basin (Pt6) and outside the basin (Pt7). It is clear that the acceleration inside the basin is greater compared to that outside. This is true in both directions. However, this amplification is different depending on the location of the seismic source. For example, the movement of point 6 is greater compared to point 7 for source 3 in the direction EW. In contrast, this same movement is more important for source 2 in the NS direction.

The amplification functions plotted on figure 5 shows the appearance of more or less significant peaks depending on the direction. It is emphasized that all the sources have the same amplitude, only their geographical coordinates are different. Here again, the location of the source has an

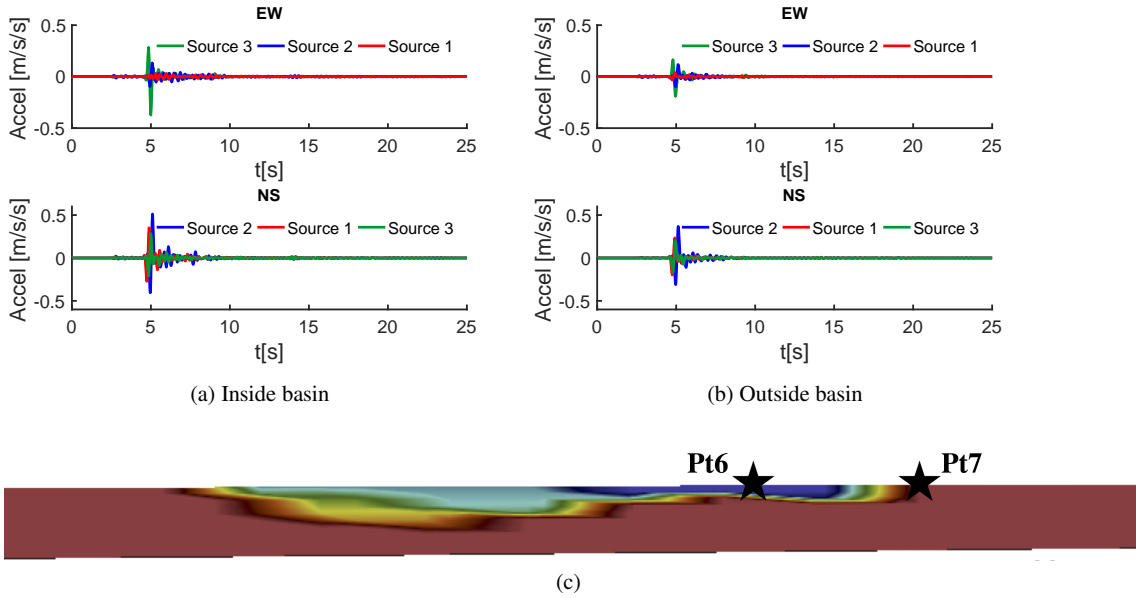


Figure 4.: Comparison of the time history acceleration of the three studied sources in EW and NS directions at the point 6 located inside the basin (Pt6) and at point 7 located outside the basin (Pt7).

effect on the peak frequency and the intensity of the amplification. Indeed, when the source is located towards the East of the basin (source 3), the peak is slightly shifted towards the high frequencies and the amplification is stronger. On the other hand, when the source is shifted towards the west of the basin (source 2), the peak is slightly shifted towards the low frequencies and the amplification is less strong compared to the other cases. Source 1 is located at the basin level.

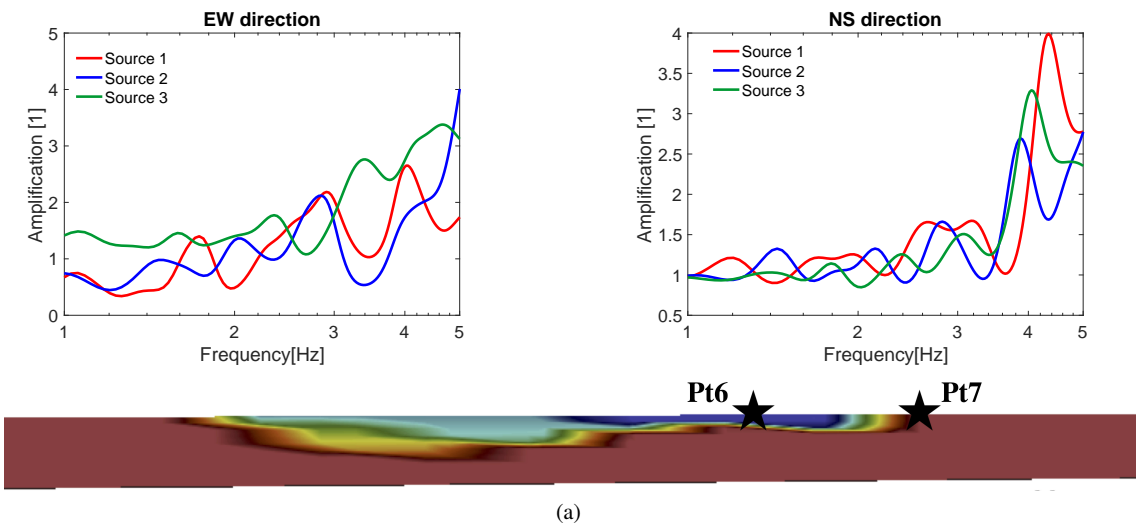


Figure 5.: Comparison of the amplification functions (spectral ratio between two time functions) of the three studied sources between receive 6 and receiver 7 in EW and NS directions

Figure 6 shows the vertical displacement function of horizontal displacement. This indicates the appearance of surface waves due to the presence of the basin. It is noted that in the NS direction the motion is stronger for the three sources while in the EW direction the motion induced by the source 1 is less strong compared to the other two cases.

Figure 7 illustrates the horizontal agitation of the receivers of interest. It shows that the movement induced by the source 1 is weak and is slightly more important in the Y direction with respect

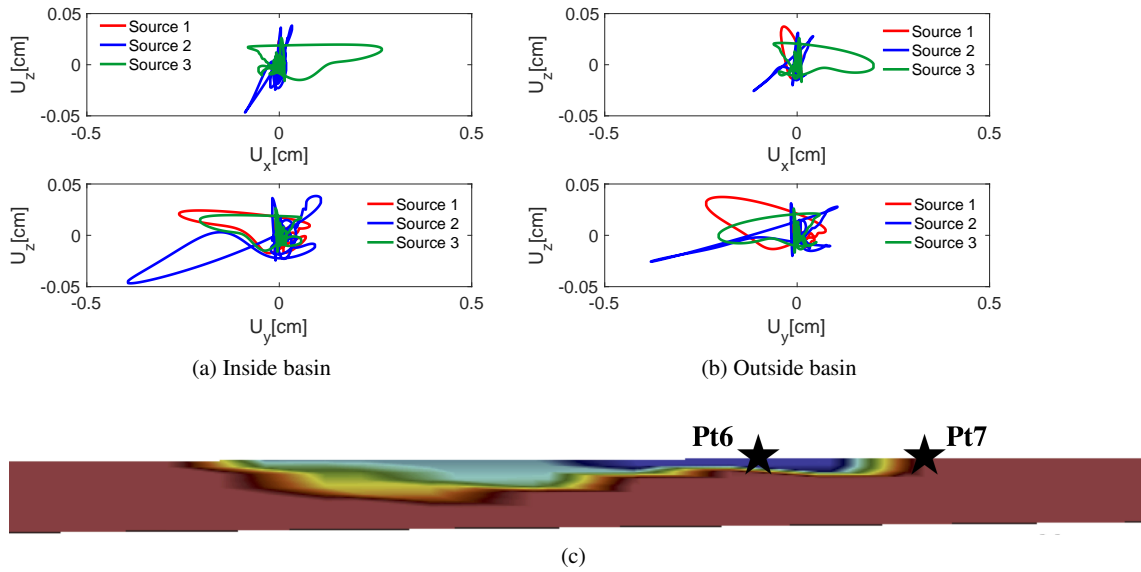


Figure 6.: Comparison of vertical displacement function of horizontal displacement in EW and NS directions of the three studied sources at the point 6 located inside the basin (Pt6) and at point 7 located outside the basin (Pt7).

to the X direction. On the other hand, sources 2 and 3 induce greater agitation. In addition, the amplitude of the motion induced by the source 2 is greater in the Y direction while the amplitude induced by the source 3 is greater in the X direction. This is true at both points.

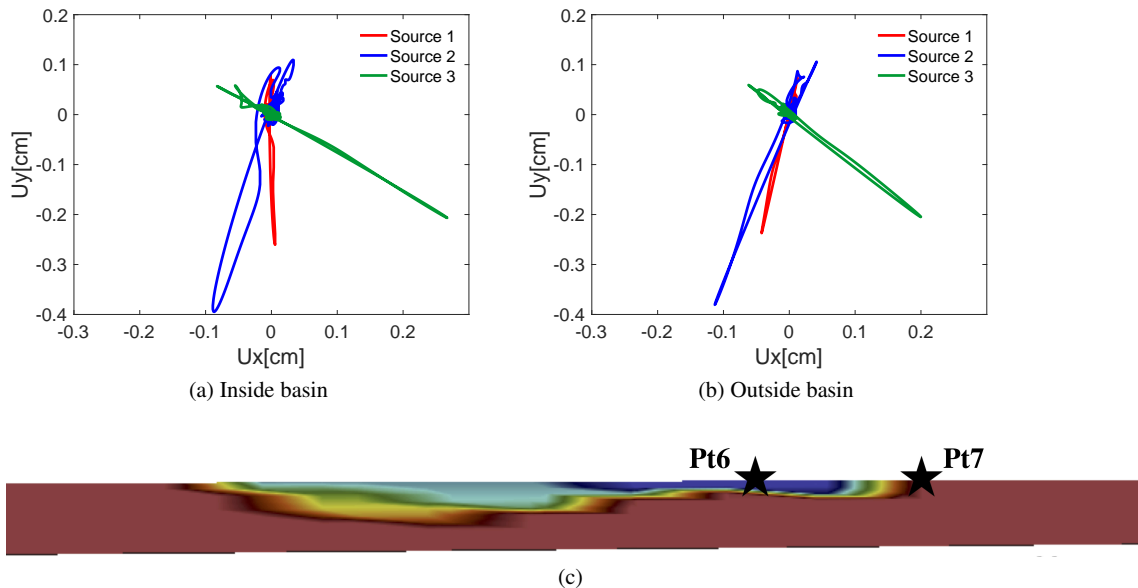


Figure 7.: Comparison of EW displacement function of NS displacement of the three studied sources at the point 6 located inside the basin (Pt6) and at point 7 located outside the basin (Pt7). The PGA values at the point 6 in EW direction are  $0.031 \text{ m/s}^2$  for source 1,  $0.13 \text{ m/s}^2$  for source 2 and  $0.36 \text{ m/s}^2$  for source 3. The PGA values at the point 7 in EW direction are  $0.033 \text{ m/s}^2$  for source 1,  $0.12 \text{ m/s}^2$  for source 2 and  $0.19 \text{ m/s}^2$  for source 3. The PGA values at the point 6 in NS direction are  $0.34 \text{ m/s}^2$  for source 1,  $0.51 \text{ m/s}^2$  for source 2 and  $0.28 \text{ m/s}^2$  for source 3. The PGA values at the point 7 in EW direction are  $0.23 \text{ m/s}^2$  for source 1,  $0.37 \text{ m/s}^2$  for source 2 and  $0.19 \text{ m/s}^2$  for source 3.



Finally, Figures 8 and 9 show that in the NS direction the location of the source has practically no influence on the response spectrum either inside or outside the basin. However in the EW direction the spectral response is modified at the sensors located in the basin. Indeed, the source 3 amplifies the response spectrum at this point.

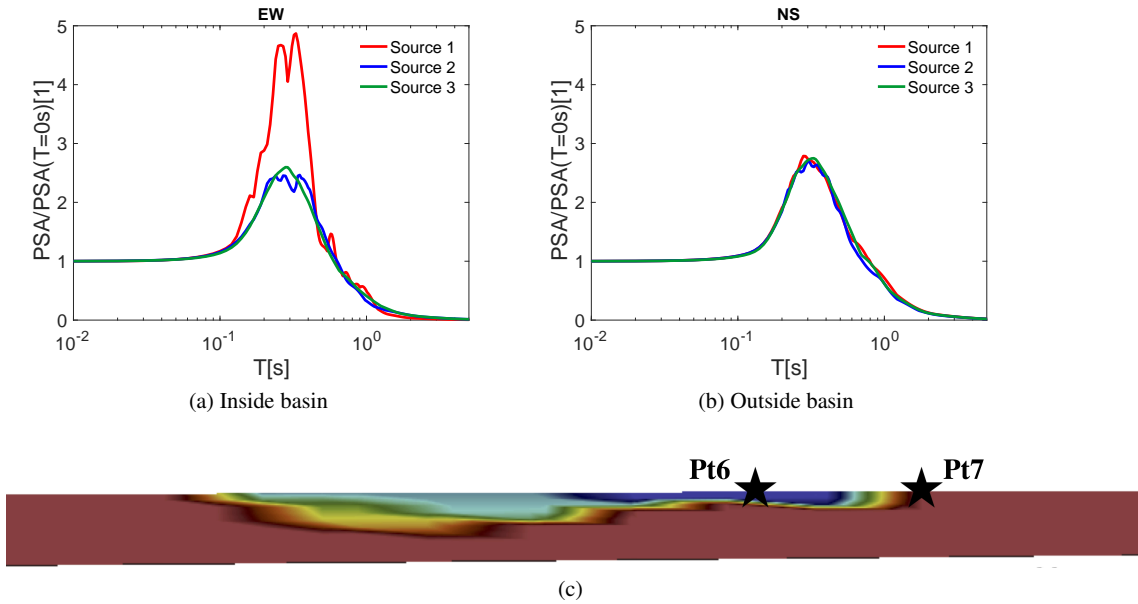


Figure 8.: Comparison of the spectrum response for the three studied sources in EW direction at point 6 located inside basin (Pt6) and at point 7 located outside the basin (Pt7). The PGA values at the point 6 in EW direction are 0.031 m/s<sup>2</sup> for source 1, 0.13 m/s<sup>2</sup> for source 2 and 0.36 m/s<sup>2</sup> for source 3. The PGA values at the point 7 in EW direction are 0.033 m/s<sup>2</sup> for source 1, 0.12 m/s<sup>2</sup> for source 2 and 0.19 m/s<sup>2</sup> for source 3.

## 5 CONCLUSION

In this paper, the effect of 3D local geology and seismic source directivity were evaluated by means of numerical simulations of regional-scale earthquake scenarios in a 0-5 Hz range. The analyses highlighted the impact of sedimentary failures that amplify the ground motion in this case study. This amplification is more or less important depending on the direction of interest. This study also highlights the influence of the location of the seismic source which could have an amplification / de-amplification effect among others.

## 6 ACKNOWLEDGEMENTS

The present work places itself within the framework of the French research project SINAPS (Séismes et Installations Nucléaires, Améliorer et Préserver la Sûreté) managed by the National Research Agency under the program Future Investments (SINAPS@ reference No.ANR-11-RSNR-0022). This project has been initiated by the members of the institute SEISM (<https://www.institut-seism.fr/en/>) after the nuclear disaster of Fukushima (Japan, 2011). It aims to enhance the scientific background in the area of the nuclear safety and radiation protection. The project contains different work packages. Our present work is part of the work package "Non-Linear Sites Effects and Soil-Structure Interaction".



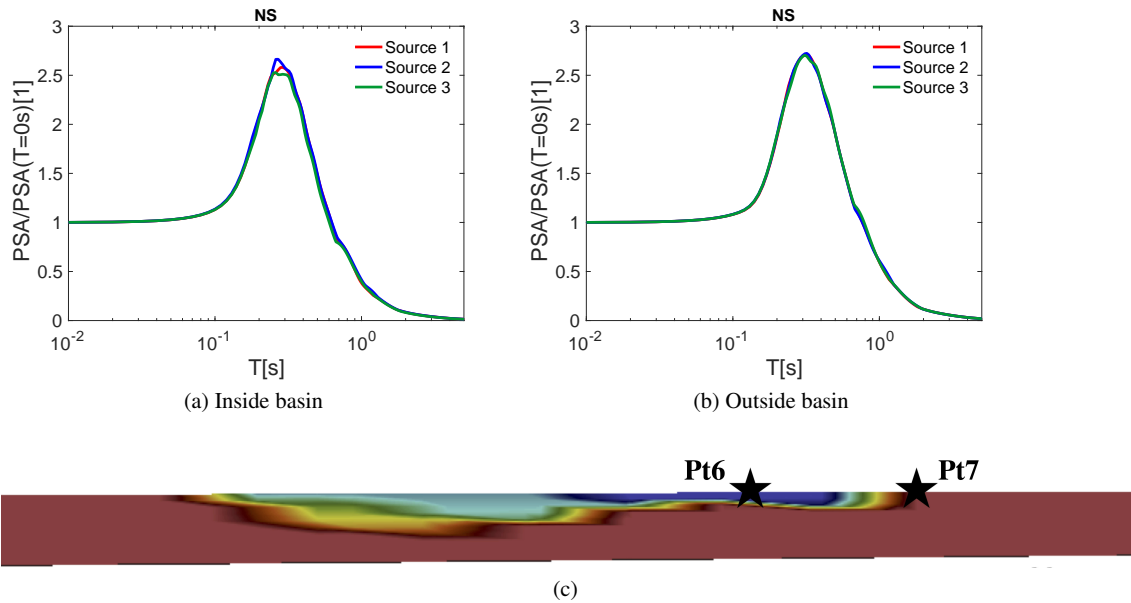


Figure 9.: Comparison of the spectrum response for the three studied sources in NS direction at point 6 located inside basin (Pt6) and at point 7 located outside the basin (Pt7). The PGA values at the point 6 in NS direction are  $0.34 \text{ m/s}^2$  for source 1,  $0.51 \text{ m/s}^2$  for source 2 and  $0.28 \text{ m/s}^2$  for source 3. The PGA values at the point 7 in EW direction are  $0.23 \text{ m/s}^2$  for source 1,  $0.37 \text{ m/s}^2$  for source 2 and  $0.19 \text{ m/s}^2$  for source 3.

## REFERENCES

- Bard, P.-Y. & Bouchon, M. 1985. The two-dimensional resonance of sediment-filled valleys. *Bulletin of the Seismological Society of America* 75(2), 519–541.
- Cruz-Atienza, V., Tago, J., Sanabria-Gómez, J., Chaljub, E., Etienne, V., Virieux, J., & Quintanar, L. 2016. Long duration of ground motion in the paradigmatic valley of Mexico. *Scientific reports* 6, 38807.
- Cushing, E., Hollender, F., Guyonnet-Benaize, C., Perron, V., Imtiaz, A., Svay, A., Bard, P., Cottureau, R., Lopez Caballero, F., Theodoulidis, N., et al. 2016. Close to the lair of odysseus cyclops: The sinaps@ postseismic campaign and accelerometric network installation on kefalonia islandsite effect characterization experiment. *Proceedings of the 7th INQUA on paleoseismology, active tectonics and archeoseismology, Crestone, Colorado, USA 30*.
- Haslinger, F., Kissling, E., Ansorge, J., Hatzfeld, D., Papadimitriou, E., Karakostas, V., Makropoulos, K., Kahle, H.-G., & Peter, Y. 1999. 3d crustal structure from local earthquake tomography around the gulf of arta (ionian region, nw greece). *Tectonophysics* 304(3), 201–218.
- Hollender, F., Perron, V., Imtiaz, A., Svay, A., Mariscal, A., Bard, P., Cottureau, R., Lopez-Caballero, F., Cushing, E., Theodoulidis, N., et al. 2015. A deux pas du repaire du cyclope d'ulysse: la campagne post-sismique et le démarrage du réseau accélérométrique sinaps@ sur île de céphalonie. In *Proceedings of the 9th AFPS National Meeting*.
- Kawase, H. 1996. The cause of the damage belt in kobe: the basin-edge effect, constructive interference of the direct s-wave with the basin-induced diffracted/rayleigh waves. *Seismological Research Letters* 67(5), 25–34.
- Louvari, E., Kiratzi, A., & Papazachos, B. 1999. The cephalonia transform fault and its extension to western lefkada island (greece). *Tectonophysics* 308(1-2), 223–236.
- Mayday, Y., Patera, A., & RBNQUIST, E. 1989. Optimal legendre spectral element methods for the multi-dimensional stokes problem. *SIAM J. Num. Anal.*
- Patera, A. T. 1984. A spectral element method for fluid dynamics: laminar flow in a channel expansion. *Journal of computational Physics* 54(3), 468–488.

- Pitarka, A., Irikura, K., Iwata, T., & Kagawa, T. 1996. Basin structure effects in the kobe area inferred from the modeling of ground motions from two aftershocks of the january 17, 1995, hyogo-ken nanbu earthquake. *Journal of Physics of the Earth* 44(5), 563–576.
- Sokos, E., Kiratzi, A., Gallovič, F., Zahradník, J., Serpetsidaki, A., Plicka, V., Janský, J., Kostelec, J., & Tselentis, G.-A. 2015. Rupture process of the 2014 cephalonia, greece, earthquake doublet (mw6) as inferred from regional and local seismic data. *Tectonophysics* 656, 131–141.
- Sokos, E., Zahradník, J., Gallovič, F., Serpetsidaki, A., Plicka, V., & Kiratzi, A. 2016. Asperity break after 12 years: the mw6. 4 2015 lefkada (greece) earthquake. *Geophysical Research Letters* 43(12), 6137–6145.